No-Reference Image Blur Assessment Based on SIFT and DCT

Shan-Qing Zhang[1], Tao Wu[2], Xiang-Hua Xu[1,*],

Zong-Mao Cheng[3], Shi-Liang Pu[4], Chin-Chen Chang[5]

[1,2,3]Hangzhou Dianzi University of Science and Technology, Hangzhou 310018, China

[4]Hikvision Company of Hangzhou,Hangzhou 310018, China

[5]Department of Information Engineering and Computer Science,

Feng Chia University, Taichung, Taiwan

[*]Corresponding author: xhxu@hdu.edu.cn

ABSTRACT. *Image blur is a key distortion that influences the image quality. In this paper, a no-reference image blur assessment method is proposed based on the scale-invariant feature transform (SIFT) and the sum of squared AC coefficients of discrete cosine transform (DCT) ,namely (SSAD). Firstly, to obtain the interested blocks in blurred image, the SIFT points are detected in its gray image. Meantime, the gradient map is also computed from gray image to obtain shape information of blurred image. Secondly, the gray image and the gradient map are both divided into equally sized blocks. The blocks in gray image containing one or more SIFT points are selected as interested blocks. The corresponding blocks in gradient map are selected to compute SSAD in DCT domain. Finally, blur score is defined as the normalized sum of SSAD by the weighted sum of cubic power entropy and variance of interested blocks, in which the weight comes from a function with the number of SIFT point as parameter.In order to verify our algorithm's performance, four public image quality databases are tested. Experimental results show that the method indeed outperforms others and the blur scores are highly consistent with subjective evaluations.*

Keywords: Image blur assessment, Gradient map, SIFT points, DCT, Entropy

1. **Introduction.** Image quality assessment (IQA) becomes very important in the modern image processing systems, such as digital camera and surveillance system. Based on the availability of the reference image, the IQA methods are classified into full-reference (FR) [**1-6**] , reduced-reference (RR) [**7-12**] , and no-reference (NR) [**13-21**][**24**] . Compared with FR and RR, NR method has better research value because of its wide applications in real world. NR IQA metrics can be further classified into distortion-specific and no-distortion-specific methods.

For image blur — a specific image distortion, researchers have proposed a lot of NR assessment methods. Wu et al.[**13**] extracted edge from blurred images by traditional edges detectors and then estimated the point spread function (PSF) from the line spread function (LSF), where LSF was constructed from the information of edges. The final blur score was computed by using the PSF. In [**14**] , Ferzli and Karam introduced the notion of just noticeable blur (JNB). The JNB was defined as a threshold with which a human can perceive blurriness around an edge . The JNB concept was used to estimate final blur scores. Narvekar et al.[**15**] presented a method based on JNB and utilized a probabilistic model to estimate the probability of detecting blur at each edge of the

image, and then blur information was pooled by computing the cumulative probability of blur detection(CPBD). Vu et al. [16] applied both spectral and spatial properties of the image .The resulting measure, S3 (Spectral and Spatial Sharpness), yields a perceived sharpness map in which greater values denote perceptually sharper regions. The blur score is computed from the sharpness map. In [17], a new method was proposed by Hassen et al. based on local phase coherence (LPC) computed on complex wavelet domain, which LPC is used to measure the blur degree. Bahrami and Kot[18] proposed a method based on the maximum local variation (MLV) , which was first computed within 8-pixel neighborhood for each pixel. Finally, the blur score is obtained by computing standard deviation of the weighted MLV distribution. In [20] , Kerouh and Amina Serir proposed a method to evaluate the blur of the image based on discrete cosine transform(DCT) and JNB metric. The edges map constructed from blurred image with JNB method was transformed to DCT domain. The degree of blur could be obtained by a machine learning system with features on DCT domain. A NR metric was proposed by Li et al.[21] based on Tchebichef-moment, which was employed to compute the sum of squared non-DC moment (SSM) values in the gradient map. SSM was shown as an effective metric in shape description. Meanwhile, for reducing the influence of image content, the sum of block variances are used to normalize SSM values. With consideration of visually salient regions, Saliency Detection by Simple Priors (SDSP) model[22] was used to compute the saliency map. The final blur score was computed by normalizing SSM with variance, which is weighted by saliency map.

Although blind image blur evaluation(BIBLE) method in[21] is effective to assess the blur, it has some disadvantages: Firstly, instead of Tchebichef-moment, DCT has nearly the same performances as Tchebichef-moment [23] , because DCT has wide applications and fast implementation. Secondly, image content are related with many factors except variance. We will use the combination of block variance and entropy to reduce the influence of image content.This will be described in Section 2.2. Lastly, SDSP model has a high time complexity.

In this paper, a novel method of NR image blur assessment is proposed, which combines the scale-invariant feature transform (SIFT) with the sum of squared AC coefficients of DCT (SSAD).Our method is motivated by [11][21][24] and makes full use of the interested regions and shape information of the blurred image. In [24] , Cai et al. proposed a novel blind blur assessment method based on feature points. The blurred and re-blurred images are both used to compute the block-wise-quantity maps, in which every pixel's value is the quantity of feature points in corresponding image block. The final blur score is the similarity between two block-wise-quantity maps. The feature points can reflect the image local information but quantity of feature points extracted from blurred images can only represent image shape changes [11] . To better use the feature points, the block containing features point and the quantity of feature points are both used here. Meantime, SIFT points used here instead of Harris feature points has more robustness because of multiscale characteristic [25] .

The performance of the proposed method is tested on four public image quality databases [6][26][27][28][31][32] . The experimental results indicate that our blur scores are much better consistent with HVS. The main contributions of this study are given as follows:

- Locating some interested blocks in gray image and corresponding blocks in gradient map with the SIFT technology, which is better close to HVS.
- Using the sum of SSAD of corresponding block in the gradient map to represent the changes of the image shape and edges.

• Employing the weighted sum of cubic power entropy and variance of a blurred image to reduce the influence of image contents.
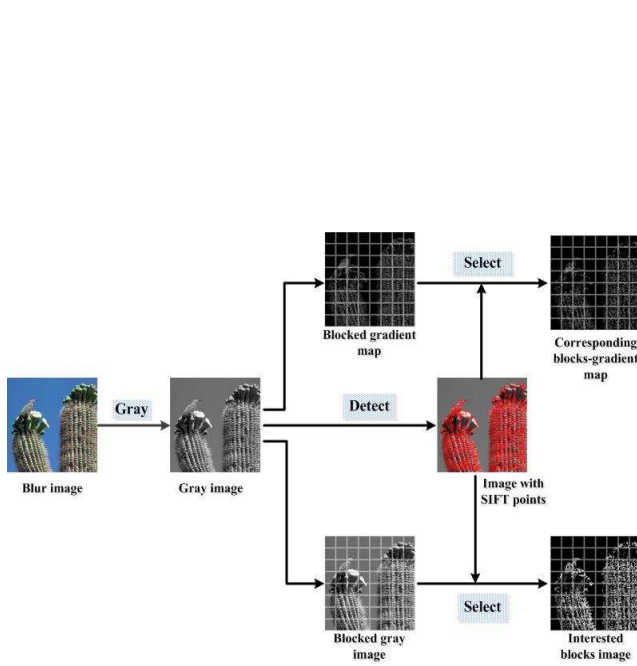

FIGURE 1. Selection of interested blocks by SIFT
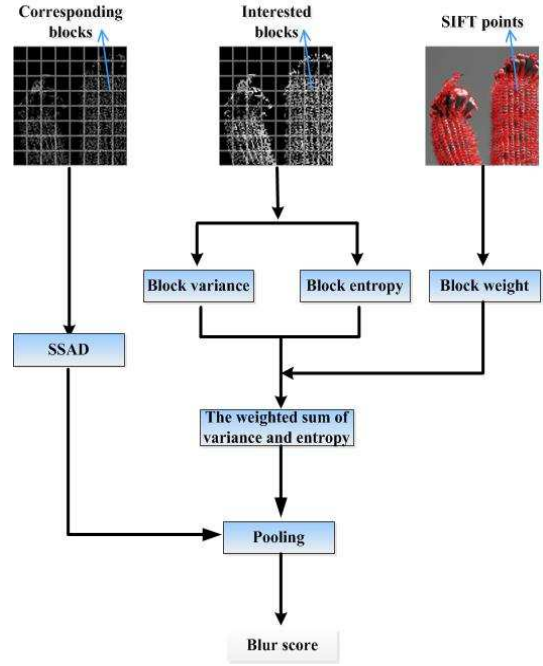
FIGURE 2. Evaluation of blur score with SSAD

2. **Algorithm.** We propose a novel blur assessment method based on the SIFT technology and DCT. The SIFT technology is used to select some interested blocks and corresponding blocks in gradient map. Meantime, to compute SSAD values, the corresponding blocks in gradient map are transformed into DCT domain. The sum of SSAD of the corresponding blocks is employed to evaluate the blur degree. The algorithm includes two phases: selection of interested blocks by SIFT and evaluation of blur score with SSAD, which are shown in Fig.1 and Fig.2. Both phases will be introduced in Subsections 2.1 and 2.2 respectively.

2.1. **Phase I—Selection of interested blocks by SIFT.**

(i) *Computing gray image and gradient map*

First of all, a blurred image is converted to the gray image I. To obtain the edges of image, the gradient map G is computed as Eq.(1):

$$G = \frac{|I_x| + |I_y|}{2},\tag{1}$$

where $I_x = \frac{\partial I}{\partial x}$ and $I_y = \frac{\partial I}{\partial y}$.

(ii) *Detecting SIFT points in gray image*

The SIFT technology is highly correlated with HVS. A saliency map can be extracted with SIFT technology in[**25**] .Therefore, SIFT technology is used to select some interested blocks.

(iii) *Selecting the interest blocks in gray image and the corresponding blocks in gradient map*

The gray image I and the gradient map G are both divided into equally sized blocks. The block size is set to be $m*n$. According to the positions of SIFT points in previous step, blocks in I containing SIFT points are selected as interested blocks, denoted by a set B_1. The corresponding blocks in G are also selected, denoted by set B_2. It is observed from Fig.3 that SIFT points always lie in the key position of an image. The interested parts of an image can be located very well while unimportant parts are eliminated successfully.

$$B_1 = \{b_{11}, b_{12}, ..., b_{1s}\}, \tag{2}$$

and

$$B_2 = \{b_{21}, b_{22}, ..., b_{2s}\}, \tag{3}$$

where b_{1x} and b_{2y} indicate an interested block in gray image and corresponding block in gradient map respectively. s is the total numbers of interested blocks. And the number of SIFT points in each block is counted to form a set A.

$$A = \{n_1, n_2, ..., n_s\}, \tag{4}$$

where n_x is the number of SIFT points in b_{1x}.
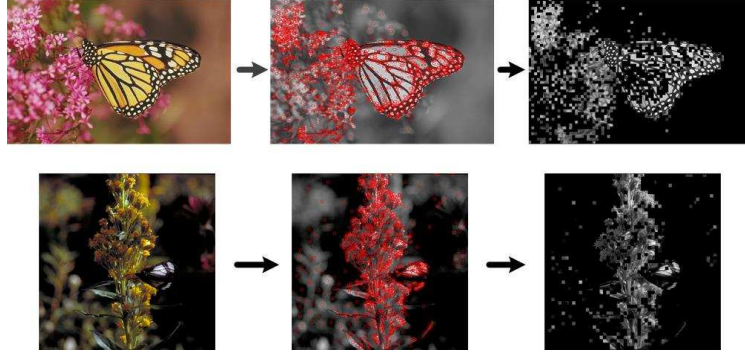
FIGURE 3. The blurred images(on left column),the images with SIFT points (on mid column) and the result images only including the interested blocks(on right column)

2.2. Phase II—Evaluation of blur score with SSAD.

(i) *Computing SSAD of a block*

Each block b_{2y} in B_2 is firstly converted into DCT domain.

$$D^y = \left\{ \begin{array}{cccc} D^y_{00} & D^y_{01} & \cdots & D^y_{0n} \\ D^y_{10} & D^y_{11} & \cdots & D^y_{1n} \\ \vdots & \vdots & \ddots & \vdots \\ D^y_{m0} & D^y_{m1} & \cdots & D^y_{mn} \end{array} \right\}, \tag{5}$$

where D^y_{00} is the DC coefficients, and the others are AC coefficients that reflect an image's edges and shapes. These AC coefficients are employed to compute SSAD value:

$$E_y = \sum_{p=0}^{m} \sum_{q=0}^{n} (D^y_{pq})^2 - (D^y_{00})^2. \tag{6}$$

In Eq.(6),E_y is SSAD value of the y-th block in B_2. As described in [8] , blur causes spread of edges and results in shape changes. The high-frequency and mid-frequency coefficient of DCT domain decrease with the increase of blur degree, which leads to a reductionship of the sum of SSAD ($\sum_{y=1}^{s} E_y$). The relation between the sum of SSAD

and Gaussian blur standard deviation for different example images is shown in Fig.4. It can be observed from Fig.4 that the sum of SSAD of an image is reduced significantly with the increase of standard deviation of Gaussian blur. Like the sum of SSM in [21] , the sum of SSAD can also be used to evaluate image blur but it is more convenient than the sum of SSM.

(ii) *Computing entropy and variance for every block*

The sum of SSAD values of an image can indicate the blur degree. However, different images have different sum of SSAD values although they are at same blur degree, as is shown in Fig.4. This may caused by different contents of different images. To obtain the identical scores, the influcence of image content must be eliminated. In [21] , variance is employed to normalize the sum of SSM to reduce influence of image contents. However, variance is one of the factors referring to image contents. Furthermore, some images with different contents might have the same variance, as shown in Fig.5. In Fig.5, two images have different contents while they have same variances indeed, where variances of(a) and (b) are both 1360.38. This indicates that only variance of an image can't eliminate influence of image's contents completely. The variance is only used to describe contrast of an image[3] .
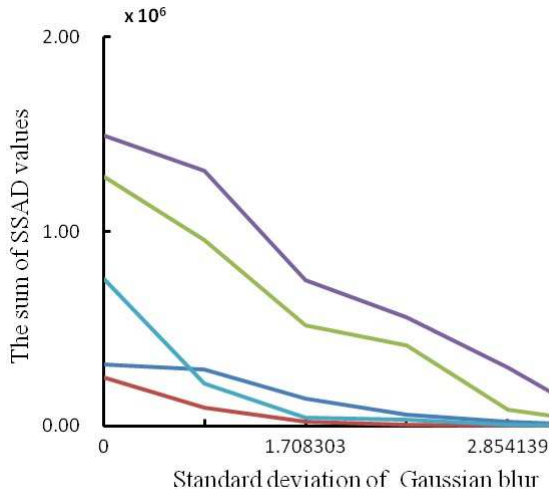

FIGURE 4. Relationship between the sum of SSAD and Gaussian blur standard deviation
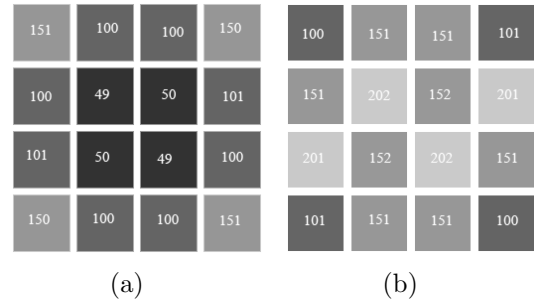

FIGURE 5. Example of two images with the same variance but different contents

In [12] , entropy is also applied to access the image quality. Different from variance, image entropy indicates its average information. Combination of entropy and variance are used to normalize the sum of SSAD to reduce influence of image contents, and better results could be obtained than the case with single variance as follows.

In the following, a combination of entropy and variance is designed as:

$$C_x = w_x(\sigma^2{}_x + h^3{}_x),\tag{7}$$

$$w_x = \frac{1}{1 + \alpha e^{n_x{}^\beta}},\tag{8}$$

$$\sigma^2{}_x = \frac{1}{mn}\sum_{i=1}^{m}\sum_{j=1}^{n}(I(i,j) - \mu)^2,\tag{9}$$

and

$$h_x = \sum_{i=1}^{256} (-p_i log p_i), p_i \neq 0. \tag{10}$$

In Eqs.(8$\sim$10), w_x is a function with parameters , in which n_x is the SIFT number of $x - th$ block in B_1, σ^2 is variance, μ indicates the mean value, h_x is the entropy. The exponential of entropy is 3, which is determined by experiments.How to determine the α and β will be introduced in Section 3.1.

(iii) *Pooling*

Finally, the sum of C_x is used to normalize the sum of E_y values in an image .The final blur score is denoted by Eq.(11):

$$score = r \times \frac{\sum_{y=1}^{s} E_y}{\sum_{x=1}^{s} C_x}, \tag{11}$$

where r is a scale factor constant. In this paper, we set $r = 0.1$.

3. Experimental results.

3.1. **Experimental settings.** Our experiment is conducted on six public image databases, including LIVE[26] , Categorical Subjective Image Quality (CSIQ)[6] , Tampere Image Database 2008 (TID2008) [27] , and Tampere Image Database 2013 (TID2013)[28] , Blurred Image Database (BID)[31] , Camera Image Database (CID2013)[32] . We select images with Gaussian blur as the test samples for each database. In LIVE and CSIQ, difference mean opinion score (DMOS) is used to indicate the degree of subjective quality, and mean opinion score (MOS) is used for TID2008 and TID2013. The numbers of images tested on four databases are 145, 150, 100, and 125, respectively.

In implementation, size of block is 6*6, parameters of weight function w_x are set with $\alpha = \sqrt{2}$ and $\beta = 20$.The Lowe's matlab source code is used to detect SIFT points, and the detailed parameters setting in detecting SIFT points can be found in[29] .
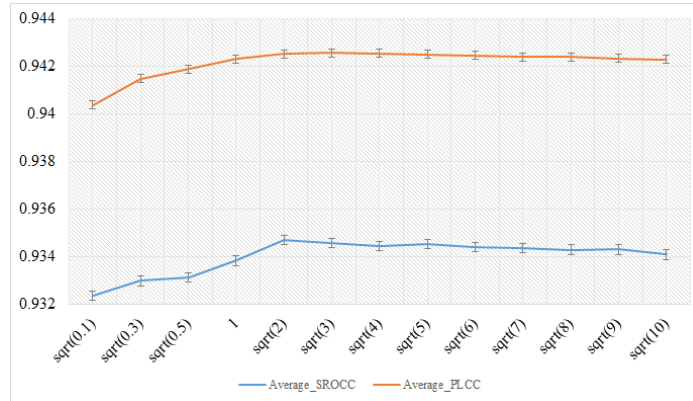
FIGURE 6. The change tendency of the weighted average PLCC and SROCC with different α.The x-axis denotes α and the y-axis denotes values of PLCC and SROCC

Compared with other methods including JNB [14] , CPBD[15] , S3[16] , LPC-SI[17] , MLV[18] and BIBLE[21] , four criterias including Pearson linear correlation coefficient (PLCC), (Kendall rank order correlation coefficient (KROCC), Spearman Rank-Order Correlation Coefficient (SROCC) and Root Mean Square Error (RMSE)[28][30] are used as reference. Higher values for PLCC, SROCC, KROCC and lower values for RMSE

indicate better performance in terms of correlation with HVS. Meantime, a logistic fitting function is commonly used to nonlinearly map between predictions and subjective scores[30] . The logistic function is given by Eq.(12):

$$f(x) = \frac{\tau_1 - \tau_2}{1 + e^{\frac{x - \tau_3}{\tau_4}}} + \tau_2,$$ (12)

where τ_1, τ_2, τ_3 and τ_4 are some parameters to be fitted.The details of this function can be refered to [30] .

In Eq.(8), we adopt a control variable method to determine α and β. When β is fixed by random selection, we adjust α to find the best correlation in LIVE database. According to this method, we firstly determine $\beta = 20$, then α can be found by computing the highest weighted average PLCC and SROCC.From Fig.6, we can find $\alpha = \sqrt{2}$ according to the highest weighted average PLCC and SROCC. The weight for each database is the number of blurred images.

3.2. **Results and analysis.**

(i) *The comparison based on images with different blur degree*

(a) DMOS=0.078 (b) DMOS=0.365 (c) DMOS=0.569

(d) DMOS=0.670 (e) DMOS=0.769 (f) DMOS=0.996
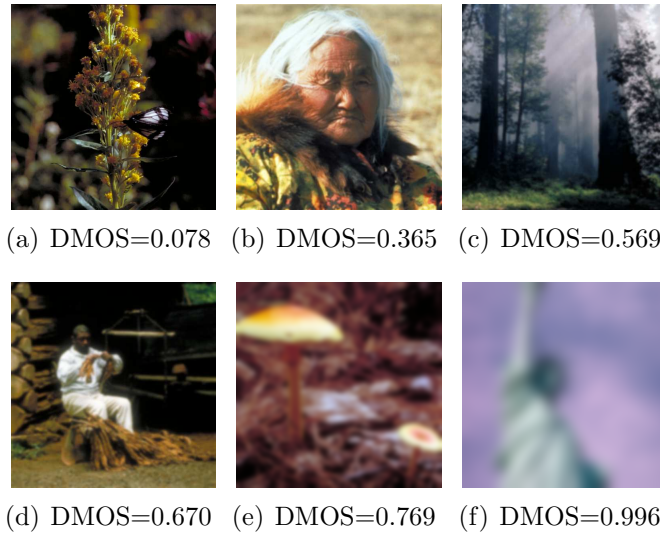
FIGURE 7. Six images with different blur degree

TABLE 1. Blur scores produced by different metrics for the images in Fig.7

Image / Metric	(a)	(b)	(c)	(d)	(e)	(f)
DMOS	0.078	0.365	0.569	0.67	0.769	0.966
JNB	1.8543	1.8048	1.6612	1.4734	1.0866	1.5132
CPBD	0.3464	0.0745	0.0178	0.006	0	0
S3	0.5119	0.0641	0.0674	0.0772	0.059	0.0224
MLV	0.1141	0.0447	0.0271	0.0339	0.0135	0.004
LPC-SI	0.9718	0.9401	0.8597	0.8578	0.4833	0.1758
BIBLE	4.5353	1.6073	1.1245	0.9417	0.2854	0.6247
OURS	1.8996	0.9567	0.644	0.6011	0.2084	0.1934

In Fig.7, six images with different blur degrees are given and the corresponding blur scores are shown in Table 1. Blur score of different metrics are described with the curves of different colors in Fig.8. With the increase of blur degree, our blur score decreases drastically and is consistent with subjective evaluations very well. However, other metrics except LPC-SI show some incorrectness. For JNB , CPBD and BIBLE, image (f) has higher DMOS than image (e) but they actually produce scores that are not consistent with DMOSs changes. S3 metric generates incorrect scores for image (b) and (c). According to changes of DMOS, blur score for image (b) generated by S3 should be greater than score for image (c). MLV has the same case between images(c) and (d). Although metric LPC-SI is consistent with the blur degree well, the interval between scores is not actually consistent with DMOS changes.
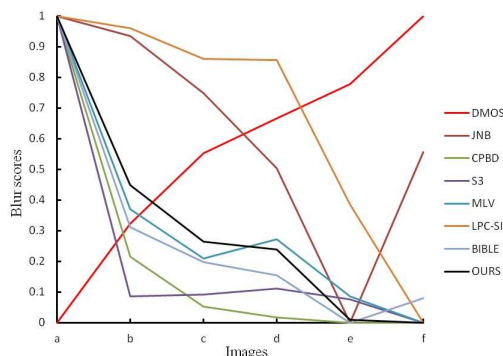
FIGURE 8. The trend of blur scores of different metrics on tested images in Fig.7

(a) DMOS=29.948	(b) DMOS=30.1402	(c) DMOS=31.0057
(d) DMOS=33.1436	(e) DMOS=34.979	(f) DMOS=36.6989
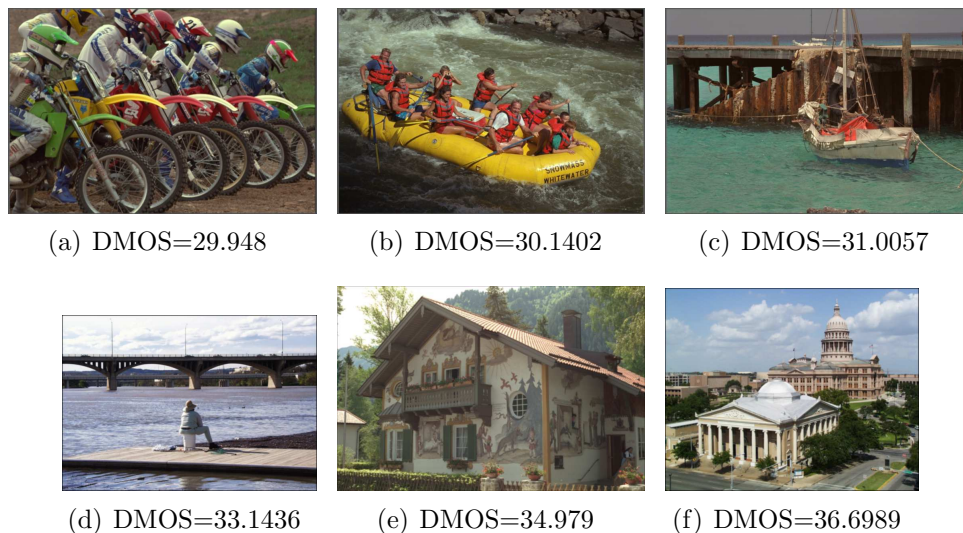
FIGURE 9. Six images with similar blur degree

(ii) *Comparison based on images with similar blur degree*

In Fig.9, six images with similar blur degree are given. The DMOS and the corresponding scores produced by six metrics are listed in Table 2. These images are randomly selected from LIVE. For HVS, the image assessment shouldn't be influenced by various images contents. From Table 2, our metric produces nearly identical scores.Compared with other methods, ours has higher accuracy and better monotonicity, and is highly consistent with HVS.

TABLE 2. Blur scores produced by different metrics for images in Fig.9

Image \\ Metric	(a)	(b)	(c)	(d)	(e)	(f)
DMOS	29.948	30.1402	31.0057	33.1436	34.979	36.6989
JNB	4.1472	4.3398	4.5699	2.862	3.8593	2.7395
CPBD	0.3273	0.3926	0.4599	0.3969	0.3902	0.3418
S3	0.1586	0.2394	0.2656	0.2622	0.1674	0.1903
MLV	0.0913	0.0939	0.0874	0.1031	0.0806	0.0857
LPC-SI	0.9571	0.9618	0.9592	0.9751	0.9543	0.9515
BIBLE	3.673	3.8631	3.588	3.4942	3.5388	3.053
OURS	1.6156	1.605	1.4822	1.4637	1.3212	1.2819

(iii) *Comparison based on databases*
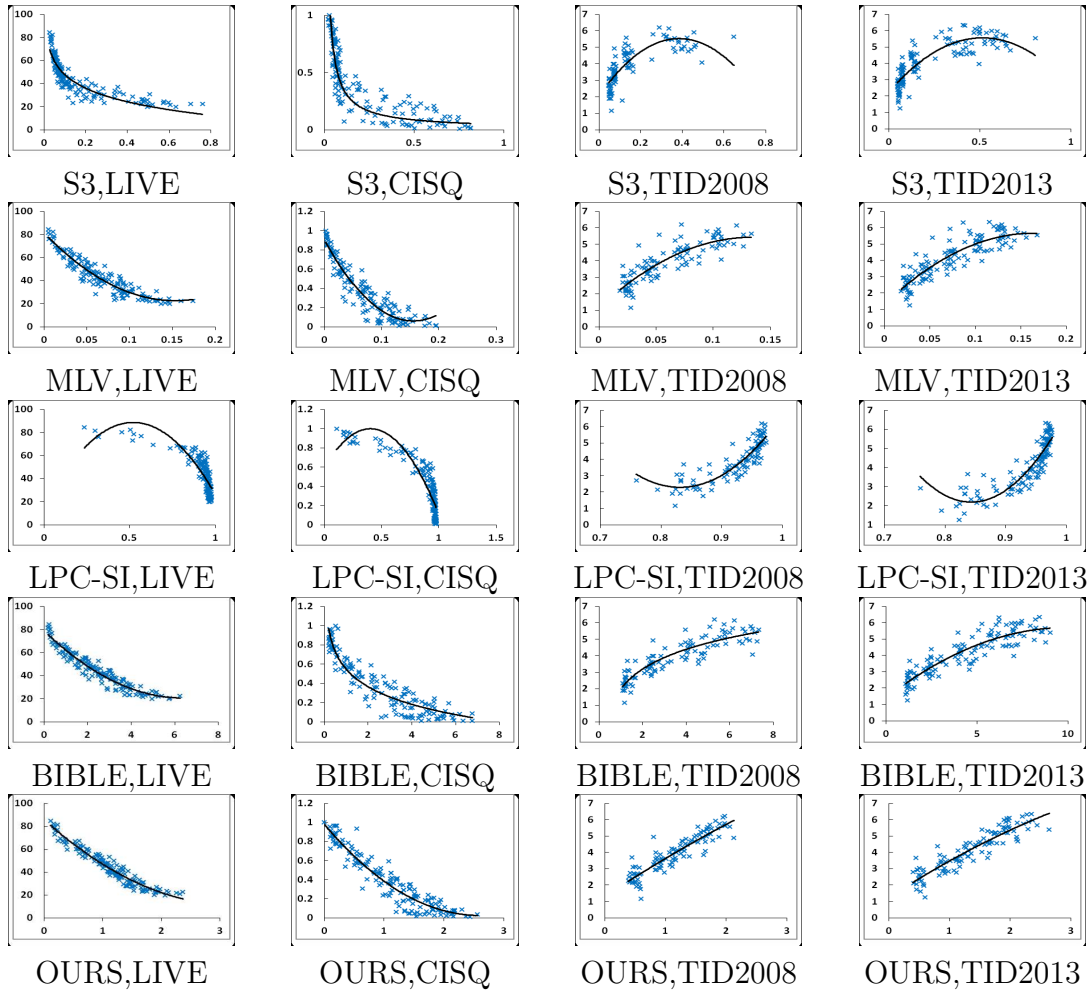
FIGURE 10. Scatter plots of subjective scores(DMOS for LIVE and CSIQ , MOS for TID2008 and TID2013) vs. blur scores produced by different methods. The x-axis represents the metric score, and y-axis represents the subjective score

In this subsection, we compare overall performance of our method with other six methods on four public image databases. In Fig.10, We show the tested results of four recent metrics: S3, MLV, LPC and BIBLE. The black curves show a trend of the fitted scatter

TABLE 3. Performance for the proposed method and six existing metrics
on artificial blur

database	criterion	JNB	CPBD	S3	LPC-SI	MLV	BIBLE	OURS
LIVE	PLCC	0.8162	0.8956	0.9436	0.9017	0.9429	**0.9622**	**0.9717**
	KROCC	0.6071	0.7652	0.8004	0.7149	0.7776	**0.8328**	**0.8538**
	SROCC	0.7877	0.919	0.9441	0.8886	0.9316	**0.9611**	**0.9709**
	RSME	9.0843	6.9929	5.2058	6.7972	5.2366	**4.2815**	**3.7167**
CISQ	PLCC	0.8061	0.8818	0.9107	0.9412	**0.9488**	0.9403	**0.9494**
	KROCC	0.5976	0.7079	0.7294	0.7683	0.7713	**0.7439**	**0.7678**
	SROCC	0.7624	0.8847	0.9059	0.7683	0.9247	**0.9265**	**0.9272**
	RSME	0.1696	0.1351	0.1184	0.0968	**0.0905**	0.0975	**0.0900**
TID2008	PLCC	0.6931	0.8235	0.8541	0.8903	0.8585	**0.8916**	**0.9101**
	KROCC	0.4951	0.631	0.6124	**0.7155**	0.6524	0.7066	**0.7381**
	SROCC	0.6667	0.8412	0.8418	**0.8959**	0.8548	0.8926	**0.9075**
	RSME	0.8459	0.6657	0.6104	0.5344	0.6018	**0.5315**	**0.4862**
TID2013	PLCC	0.7113	0.8552	0.8813	0.8197	0.8827	**0.8997**	**0.9264**
	KROCC	0.5137	0.6467	0.6397	**0.7479**	0.681	0.7071	**0.7479**
	SROCC	0.6902	0.8518	0.8609	**0.9191**	0.8787	0.8941	**0.9243**
	RSME	0.8771	0.6467	0.5896	0.7148	0.5865	**0.5448**	**0.4699**
Weighted average	PLCC	0.7644	0.8680	0.9019	0.8912	0.9139	**0.9273**	**0.9430**
	KROCC	0.5604	0.6944	0.7051	0.7384	0.7285	**0.7527**	**0.7813**
	SROCC	0.7337	0.8780	0.8934	0.8626	0.9021	**0.9180**	**0.9350**
	RSME	2.9551	2.2724	1.7449	2.1979	1.7430	**1.4552**	**1.2575**

TABLE 4. Performance for the proposed method and six existing metrics
on real blur

database	criterion	JNB	CPBD	S3	LPC-SI	MLV	BIBLE	OURS
BID	PLCC	0.2612	0.2704	**0.4271**	0.3901	0.3643	0.3165	**0.3018**
	SROCC	0.2383	0.2717	**0.4253**	0.3161	0.3236	0.3606	**0.2935**
	RSME	1.2085	1.2053	**1.1320**	1.1528	1.1659	1.1876	**1.1935**
CID2013	PLCC	0.5373	0.5245	0.6863	**0.7031**	0.6890	0.6943	**0.6770**
	SROCC	0.4511	0.4448	0.6460	0.6024	0.6206	**0.6888**	**0.6685**
	RSME	19.2699	19.4530	16.6190	**16.2474**	16.5594	16.4794	**16.853**

plots. It is observed from Fig.10 that our method has somewhat similar result with MLV
and BIBLE on four databases. S3 and ours have nearly the same results in LIVE and
CISQ database, but ours outperforms S3 on other two databases. LPC-SI shows different
fitting properties. Although it is closest to BIBLE on four databases, it produces the best
fitting results because scatter points are more densely clustered around the fitted curve.
For all of four databases, our method shows better performance than others, which has
better adaptability and stability.

Using four criteria: SROCC, KROCC, PLCC and RMSE, some comparison results
between our method and others on all four public image databases are listed in Table 3.
We mark the best results among all methods in black boldface. In Table 3, the proposed
method has the best results on all of four databases. Although our method has somewhat
similar results with BIBLE in LIVE and MLV in CISQ, respectively, it has much better
results on other two databases. Meanwhile, the average value of four criterions in last row

TABLE 5. Average values of four criteria for different block sizes

size	SROCC	PLCC	KROCC	RMSE
4x4	0.9234	0.922	0.7629	1.5263
6x6	0.9350	0.7813	0.9430	1.2575
8x8	0.9298	0.9377	0.7727	1.4054
10x10	0.921	0.9382	0.7711	1.3985
12x12	0.9292	0.9371	0.7708	1.3845

TABLE 6. Average computational time tested in CISQ database

Metric	JNB	CPBD	S3	LPC-SI	MLV	BIBLE	OURS
Time(second)	0.52	0.35	22.15	0.87	0.091	2.98	1.34

also indicates that our method has the best overall performance in terms of accuracy and monotonicity.

The blurred image of four databases in Table.3 is generated based on Gaussian low-pass filtering. In order to test our algorithm for real blur images, some experiments are conducted on BID and CID2013 databases.The results are listed in Table.4. It is observed that although our algorithm is not the best,it has nearly similar perfermance with BIBLE.

3.3. **Determination of block size.** In order to determine block size, we compute the weighted average results of SROCC, KROCC, PLCC and RMSE, which are listed in Table 5. It is observed that the best results for four criteria are obtained when block size is 6x6. Therefore, the block size is set to be 6x6 in experiments.

3.4. **Run-time estimation.** In order to test running time, experiment is conducted on CISQ database, including 150 images with size 512x512. The average time of detecting SIFT points is 1.93 second per image. The SIFT code is the Lows executed program and it includes not only detecting the SIFT points but also computing the feature descriptors.Considering this, the final average computational time will be computed by subtracting the half of 1.93s.The running time of our metric and precious methods is listed in Table 6. From the Table, the MLV metric is the fastest while the S3 metric is the lowest. Although the proposed method is not the best one compared with others, it is also not the worst.

4. **Conclusion.** In this paper, we propose a new blur assessment method combining the SIFT points and DCT. By selecting some interested blocks with SIFT technology in gray image, the sum of SSAD in gradient map is computed to evaluate the image blur degree. To reduce influence of image content, a normalized strategy for the sum of SSAD is designed by combining image entropy and variance. The experiments indicate that the normalized sum of SSAD is a better metric for image blur assessment. Our blur scores are highly consistent with HVS than previous methods. Moreover, experiments illustrate that the proposed method has better accuracy and stronger monotonicity.

References

[1] Z. Wang, A. C. Bovik, H. R. Sheikh, E. p.Simoncelli, Image quality assessment: from error visibility to structural similarity, *IEEE Transactions on Image Processing*, vol.13, no.4, pp.60012, 2004.

[2] L. Zhang, D. Zhang, X. Mou, Fsim: A feature similarity index for image quality assessment, *IEEE Transactions on Image Processing*, vol.20, no.8, pp.23782386, 2011.

[3] Z. Wang, E. P. Simoncelli, A. C.Bovik, Multi-scale structural similarity for image quality assessment, *Proc. Proceedings of the 37th IEEE Asilomar Conference on Signals, Systems and Computers, Pacific Grove, CA*, pp.912, 2003.

[4] H. Z. Nafchi, A. Shahkolaei, R. Hedjam, M. Cheriet, Mean deviation similarity index: Efficient and reliable full-reference image quality evaluator, *IEEE Access*, vol.4, no.99, pp.55795590, 2016.

[5] A. Liu, W. Lin, M. Narwaria, Image quality assessment based on gradient similarity, *IEEE Transactions on Image Processing A Publication of the IEEE Signal Processing Society*, vol.21, no.4, pp.15001512, 2012.

[6] E. C. Larson, D. M. Chandler, Most apparent distortion: full-reference image quality assessment and the role of strategy, *Journal of Electronic Imaging*, vol.19, no.1, pp.011006, 2010.

[7] D. Tao, X. Li, W. Lu, X.Gao, Reduced-reference IQA in contourlet domain, *IEEE Transactions on Systems Man & Cybernetics Part B Cybernetics A Publication of the IEEE Systems Man Cybernetics Society*, vol.39, no.6, pp.16237, 2009.

[8] P. Marziliano, F. Dufaux, S. Winkler, T. Ebranhimi, Perceptual blur and ringing metrics: application to jpeg2000, *Signal Processing Image Communication* vol.19, no.2, pp.163172,2004;.

[9] G Chen, S Coulombe, An Image Visual Quality Assessment Method Based on SIFT Features, *Computer Engineering*, vol.1, no.1, pp.85-97, 2013.

[10] Z. Wang, A. Bovik, Modern image quality assessment, *Synthesis Lectures on Image Video & Multimedia Processing*,vol.2, no.1 pp.156, 2006.

[11] T. Sun, S. Ding, W.Chen, Reduced-reference image quality assessment through sift intensity ratio, *International Journal of Machine Learning and Cybernetics*, vol.5, no.6, pp.923931,2014.

[12] S. Wang, X. Zhang, S. Ma, W. Gao, Reduced reference image quality assessment using entropy of primitives, *Proc. Picture Coding Symposium*, pp.193196, 2013.

[13] S. Q. Wu, W. S. Lin, S. xie, Z.Lu, E. P. Ong, S. S. Yao, Blind blur assessment for vision-based applications, *Journal of Visual Communication Image Representation* , vol.20, no.4, pp.231241, 2009.

[14] R.Ferzli, L. J. Karam, A no-reference objective image sharpness metric based on the notion of just noticeable blur (JNB), *IEEE Transactions on Image Processing*, , vol.18, no.4, pp.717728, 2009.

[15] N. D. Narvekar, L. J. Karam, A No-Reference Image Blur Metric Based on the Cumulative Probability of Blur Detection (CPBD), *IEEE Trans Image Process*, vol.20, no.9, pp. 2678-2683, 2011.

[16] C. T. Vu, T. D. Phan, D. M. Chandler, S3:a spectral and spatial measure of local perceived sharpness in natural images, *IEEE Transactions on Image Processing*, vol.21, no.3, pp.934945, 2012.

[17] R. Hassen, Z. Wang, M. M. A, Sslama, Image sharpness assessment based on local phase coherence, *IEEE Transactions on Image Processing*, vol.22, no.7, pp.2798, 2013.

[18] K. Bahrami, A. C. Kot, A fast approach for no-reference image sharpness assessment based on maximum local variation, *IEEE Signal Processing Letters*, vol.21, no.6, pp.751755, 2014.

[19] J. Guan, W. Zhang, J. Gu, H. Ren, No-reference blur assessment based on edge modeling, *Journal of Visual Communication Image Representation*, vol.29, no.C, pp.17, 2015.

[20] F. Kerouh, A. Serir, Perceptual blur detection and assessment in the dct domain, *Proc. International Conference on Electrical Engineering*, pp.14, 2015.

[21] L. Li, W. Lin, X. Wang, G.Yang, No-reference image blur assessment based on discrete orthogonal moments, *IEEE Transactions on Cybernetics*, vol.46, no.1, pp.3950, 2016;

[22] L. Zhang, Z. Y. Gu, H. Y. Li, SDSP: A novel saliency detection method by combining simple priors, *Proc. IEEE Conf. Image Process. (ICIP), Paris, France*, pp.171175, 2013.

[23] R Mukundan, Transform coding using discrete Tchebichef Polynomials,*Acta Press*, 2006.

[24] H. Cai, L. D. Li, L. Li*, J. Qian, Image blur assessment with feature points, *Journal of Information Hiding and Multimedia Signal Processing*, vol.6, pp.20734212, 2015.

[25] L. Li, W. Xia, W. Lin, Y. Fang, S. Wang, No-Reference and Robust Image Sharpness Evaluation Based on Multiscale Spatial and Spectral Features, *IEEE Transactions on Multimedia*, vol.19, no.5, pp.1030-1040, 2017.

[26] H. R. Sheikh, M. F. Sabir, A. C. Bovik, A statistical evaluation of recent full reference image quality assessment algorithms, *IEEE Transactions on Image Processing A Publication of the IEEE Signal Processing Society*,vol.15, no.11, pp.44051, 2006.

[27] N. Ponomarenko, V. Lukin, A. Zelensky, K. Egiazarian, M. Carli, F. Battisti, Tid2008 - a database for evaluation of full-reference visual quality assessment metrics, *Adv Modern Radioelectron*, vol.10, pp.3045, 2004.

[28] Nikolay, Ponomarenko, Oleg, Ieremeiev, V. Lukin, K. Egiazarian, L.Jin, J. Aea. Color image database tid2013: Peculiarities and preliminary results. *Proc. European Workshop on Visual Information Processing*, pp.106111, 2013.

[29] D. G. Lowe, Distinctive image features from scale-invariant key-points, *International Journal of Computer Vision*, vol.60, no.2, pp.91110, 2004.

[30] Final report from the video quality experts group on the validation of objective models of video quality assessment. http://www.vqeg.org ,2003.

[31] T. Virtanen, M. Nuutinen, M. Vaahteranoksa, P. Oittinen, and J. Hakkinen, CID2013: A database for evaluating no-reference image quality assessment algorithms", *IEEE Trans. Image Process*, vol.24, no.1, pp.390402, 2015.

[32] A. Ciancio et al, No-reference blur assessment of digital pictures based on multifeature classifiers", *IEEE Trans. Image Process*, vol.20, no.1, pp.6475, 2011.